J Solid State Electrochem (1997) 1: 199–207

ORIGINAL PAPER

C. Guéry · C. Choquet · F. Dujeancourt · J.M. Tarascon
J.C. Lassègues

Infrared and X-ray studies of hydrogen intercalation in different tungsten trioxides and tungsten trioxide hydrates

Received: 5 March 1997 / Accepted: 21 May 1997

Abstract Hydrogen intercalation via spillover reaction in various tungsten trioxides leads to the formation of blue hydrogen bronzes. These reversible reactions induce changes in the W—O bond system while maintaining the W—O skeleton. The effect of the intercalation process on the host crystalline structure has been studied with respect to the ν(O—W—O) stretching vibration changes and lattice parameter variations by means of infrared and X-ray diffraction measurements. Among the main results, the intercalation process is shown to be strongly influenced by the structural type of the host compound as well as its amorphous versus crystalline nature. For instance, for the ReO_3 type oxides (monoclinic and cubic WO_3) and hexagonal WO_3, ν(O—W—O) shifts to higher frequency are assigned to a shortening effect of W—O bonds. A W—O bond system arrangement is also measured for the crystallized and amorphous hydrates $WO_3 \cdot H_2O$, but no detectable changes could be found in the pyrochlore WO_3 and in the hydrate $WO_3 \cdot 1/3\ H_2O$.

Key words Tungsten trioxides · Tungsten trioxide hydrates · Hydrogen intercalation · X-ray powder diffraction · Infrared spectroscopy

Introduction

The WO_3 tungsten oxides are well known for their electrochromic properties [1]. Upon reversible intercalation of light ions such as protons or lithium according to the following reaction, $WO_3 + xM^+ + xe^- \leftrightarrows M_xWO_3$ with M = H or Li, the most noticeable effect is the color change from white (oxides) to dark blue (bronzes). This intercalation reaction usually induces some W—O bond distortions while preserving the basic W—O skeleton. Many studies have dealt with the hydrogen intercalation into tungsten oxides, and the relationship between their structural and physical properties has been much discussed [2–9]. Nevertheless, the fundamentals of the intercalation phenomenon are still a subject of controversy. The study of intercalation on well-characterized "model WO_3 phases" thus appears necessary to better understand the exact role of the W—O skeleton and the WO_3 structural type.

Previous infrared spectroscopy studies on WO_3 thin films have identified O—H bonds within W—O—H groups, implying that the intercalation reaction occurs according to: $O_2W^{6+} = O + xH^+ + xe^- \leftrightarrows O_2W^{5+}—O—H_x$ [2, 3]. This was confirmed by powder neutron diffraction studies performed on different crystalline tungsten or molybdenum oxides, have shown the presence of O—H bonds (of about 1.1 Å) implicated in metal-OH groups. However, the exact position of the intercalated protons could not be determined from such measurements; it was assumed that they were statistically distributed among either the 48 equivalent crystalline positions in the cubic hydrogen tungsten bronze $H_{0.53}WO_3$ [4] or the bridging oxygens in the lamellar orthorhombic molybdenum bronze $H_{0.34}MoO_3$ [5]. Because of the existence of O—H bonds, the formulation of the bronzes was then re-written $WO_{3-x}(OH)_x$ and $MoO_{3-x}(OH)x$ (oxyhydroxides of tungsten or molybdenum). In the latter case, the existence of Mo—O—H groups was confirmed by establishing the presence of a bending vibration band at 1267 cm^{-1} by inelastic neutron scattering [5]. NMR studies of hydrogen intercalation compounds of hexagonal WO_3 supposed the presence of O—H bonds as well [6]. Other intercalation studies performed on different cubic bronzes M_xWO_3 with M = Li, Na and La have shown an increase both

C. Guéry (✉) · C. Choquet · F. Dujeancourt · J.M. Tarascon
Laboratoire de Réactivité et de Chimie des Solides,
UPRES-A 6007, Université de Picardie Jules Verne,
Faculté des Sciences, 33 rue Saint Leu, 80039 Amiens Cédex, France,
Tel.: + 33 3 22 82 76 04; Fax: +33 3 22 82 75 90;
e-mail: claude.guery@sc.u-picardie.fr

J.C. Lassègues
Laboratoire de Spectroscopie Moléculaire et Cristalline,
URA CNRS 124, Université de Bordeaux I,
351 cours de la libération, 33405 Talence Cédex, France

in the unit cubic parameter and in W—O distances upon metal intercalation [7] (together with a release of WO_6 distortions as evidenced by structural and vibrational measurements). Finally, Mo—O—H groups have also been identified in the lamellar hydrates of molybdenum oxide bronzes $H_1MoO_3{\cdot}xH_2O$ ($x = 1$ or 2) by infrared spectroscopy, the protons being connected to the bridging oxygen of the crystalline structures [8]. However, an infrared transmission study performed on sputtered WO_3 thin films has not shown any evidence of the intercalated protons as W—O—H groups [9]. This study rather stressed the proton insertion effect on the W—O—W system as lengthening and shortening of W—O bonds.

The aim of this work is to throw some light on the understanding of the hydrogen intercalation reactions in different polymorphic forms of WO_3: monoclinic (referred to as m-WO_3), hexagonal (h-WO_3), pyrochlore (p-WO_3) and cubic (c-WO_3), and in different hydrates: crystallized $WO_3{\cdot}1\ H_2O$ and $WO_3{\cdot}1/3\ H_2O$ and an amorphous hydrate (a-$WO_3{\cdot}1\ H_2O$). Several of these phases, whose structure consists of corner-shared WO_6 octahedra, have been synthesized and characterized in our laboratory. An infrared transmission study has previously given a clear spectral identification of m-WO_3, h-WO_3, $WO_3{\cdot}1\ H_2O$, and $WO_3{\cdot}1/3\ H_2O$, showing their specific spectral distribution in the O—W—O frequency range, the short W—O bonds having a specific band around 950 cm^{-1} [10]. More specifically, we have monitored by *in situ* infrared spectroscopy and X-ray diffraction measurements the hydrogen intercalation reaction. The crystalline nature was found to mainly govern the amount of hydrogen uptake as well as the mechanism of intercalation.

Experimental

Synthesis of the precursors

The precursor phases for the present study have been prepared via soft chemistry routes according to methods previously described. The yellow monohydrate $WO_3{\cdot}1\ H_2O$ was prepared according to Freedman's method [11]. Its dehydration at 235 °C for about 25 min leads to a poorly crystallized c-WO_3 metastable oxide. By increasing the temperature to 350 °C, the stable oxide m-WO_3 is obtained. The c-WO_3 was previously observed by X-ray thermodiffractometry between 200 °C and 300 °C using $WO_3{\cdot}1\ H_2O$ as precursor [12, 13] and by electron diffractometry [14]. Differential thermal analysis [12] showed a weak transition energy of about 0.6 $kcal \cdot mol^{-1}$ corresponding to the c-WO_3 to m-WO_3 transformation, meaning that isolating the c-WO_3 phase is difficult. A narrow range of temperatures, between 230 °C and 270 °C, and a short reaction time were necessary to prepare a few milligrams of poorly crystallized solid.

$WO_3{\cdot}1/3\ H_2O$ hydrate was prepared by hydrothermal treatment at 120 °C from an aqueous suspension of a tungstic acid gel prepared according to Zocher's method [15, 16]. Its dehydration at 290 °C under an air flow leads to the metastable hexagonal oxide h-WO_3 [17]. The preparation of p-WO_3 was in accordance with [18], using ammonium paratungstate $(NH_4)_{10}\ (H_2W_{12}O_{42}){\cdot}4H_2O$ as the starting material.

The amorphous a-$WO_3{\cdot}1\ H_2O$ oxide was obtained by mechanical grinding of the monohydrate $WO_3 \cdot 1\ H_2O$ for about 14 h according to [19]. The grinding effect is to highly disorganize the crystalline structure, leading to a compound which is amorphous (as determined by X-ray diffraction). Thermogravimetric analysis has shown that this amorphous oxide retains the same amount of water as its crystallized precursor.

Hydrogen intercalation

The hydrogen intercalation in the different compounds was carried out using the spillover method [20, 21]. This consists in introducing some fine platinum particles inside a powder sample to catalyse the hydrogen intercalation reaction. The hydrogen intercalation, for example the formation of blue tungsten oxide bronzes, takes place in the platinized WO_3 by passing hydrogen through it at room temperature for several hours. A previous study has shown that adsorbed water favors the intercalation reaction [22], which has been confirmed in h-WO_3 [17]. The present intercalation experiments were carried out by outgassing the samples, which were stored in an oxygen- and water-free glove box because of the extreme sensitivity of the hydrogen bronzes to atmospheric oxygen. The hydrogen intercalation content "x" was determined by redox titration using the Kiss and Tisza method [23].

Experimental techniques

Infrared spectra were recorded on a Nicolet FTIR 510 spectrometer working in the 4000–400 cm^{-1} spectral range using a classical transmission configuration. The resolution was 4 cm^{-1}, and 32 scans were accumulated. Because of their extreme sensitivity to atmospheric oxygen, the WO_3-type bronzes deposited on a silicon window were placed inside a SPECAC hermetic cell closed by two KBr windows and flushed under an argon atmosphere. To prepare the sample for infrared, the bronze powder was first mixed with acetone with a gentle grinding, and the suspension was then deposited on the silicon window. After evaporation of the acetone, a thin layer of sample was laid on the silicon substrate. These steps were carried out in an air- and oxygen-free glove box to avoid partial reoxidation of the bronzes. Afterwards, the cell was put inside the spectrometer, and, by progressively introducing air, we were able to follow the reoxidation steps. The quality of the infrared spectra was mainly governed by the homogeneity of the deposit. The most important changes were detected in the 1000–400 cm^{-1} frequency range. This is why we have reported here all the spectra between 1100 cm^{-1} and 400 cm^{-1}. These spectra were corrected by use of a sloping base line.

The X-ray diffraction measurements on the starting and the intercalated materials were performed on a X-ray multichannel Inel diffractometer with the capillary configuration, which allowed us to study air-sensitive samples. Lindemann tubes were filled with powder samples and sealed in the glove box. The X-ray diagrams were obtained after an accumulation time of 1 h. Refinements of the corresponding cell parameters were made with a least-square fit programme. Both X-ray and infrared measurements were performed on samples of known hydrogen content.

Results

The tungsten oxides and the tungsten oxide hydrates

Before giving the experimental results and their analysis, it seems useful to recall the different crystalline structures (Fig. 1a–f) and their infrared characteristics

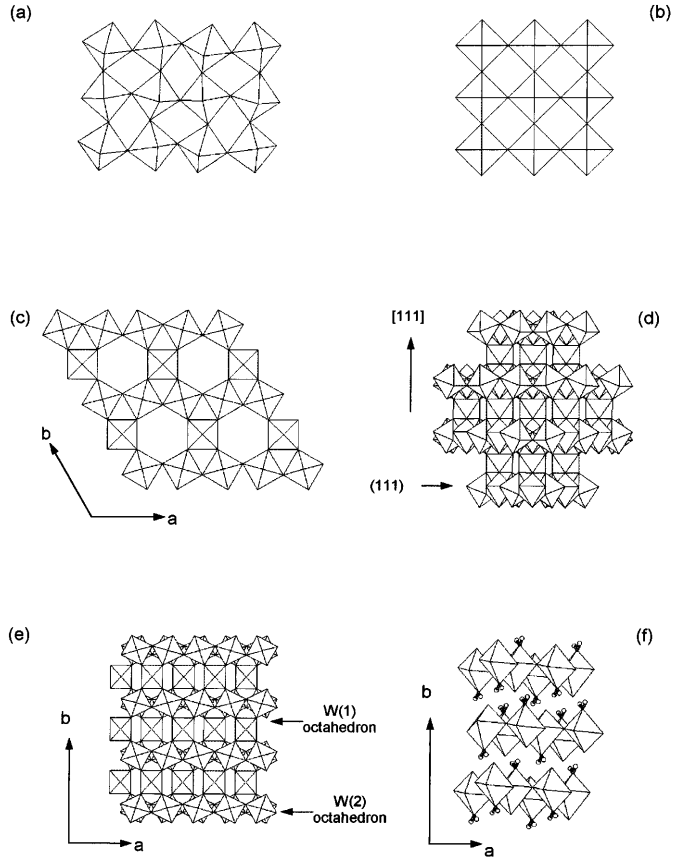

Fig. 1a–f Schematic representation of the crystalline structures of the studied compounds: **a** m-WO_3, **b** c-WO_3, **c** h-WO_3, **d** p-WO_3, **e** $WO_3{\cdot}1/3\ H_2O$, **f** $WO_3{\cdot}1\ H_2O$

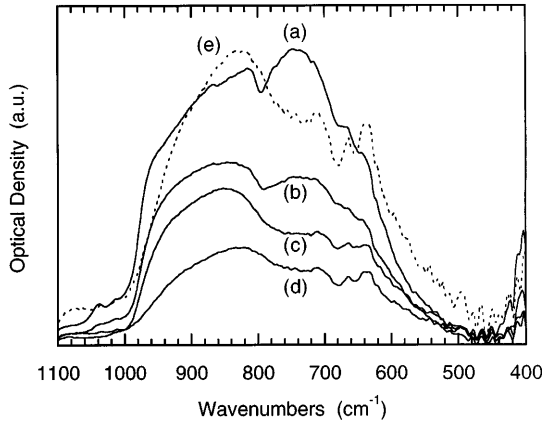

Fig. 2 Infrared spectra of monoclinic WO_3 (**a**) and of its H_xWO_3 bronzes with $x = 0.33$ (**d**) and intermediate hydrogen contents (**b** and **c**). Spectrum **e** corresponds to an amplification of **d** for convenient profile comparison with **a**

(Figs. 2–8, Spectra a), which are consistent with the previous reports. In general, the tungsten oxide structures consist of packed corner-sharing WO_6 octahedra. The corresponding tungsten oxide vibrations are characterized by three main infrared regions [10]: 900–600 cm^{-1}, 400–200 cm^{-1} and $< 200\ cm^{-1}$, which correspond to ν(O—W—O) stretching modes, bending modes and lattice modes, respectively. In this work, we have focused on the stretching vibration region, where the tungsten oxides are generally characterized by a broad absorption band. We have reported in Table 1 the structural characteristics of the different compounds and in Table 2 their stretching vibration frequencies.

The stable monoclinic WO_3 oxide (m-WO_3, Fig. 1a) has a distorted ReO_3-type structure consisting of a three-dimensional network of WO_6 octahedra [24, 25]. The metastable cubic WO_3 (c-WO_3, Fig. 1b) can be described as a non-distorted ReO_3-type structure [12–14]. The infrared spectrum of m-WO_3 (Fig. 2a) shows a large band with two maxima at 740 cm^{-1} and 810 cm^{-1}, while c-WO_3 has one band around 740 cm^{-1} (Fig. 3a). Note also for c-WO_3 the presence of some small features at 940 cm^{-1} and 980 cm^{-1} in the short-bond vibration frequency range, in relation to the poorly crystallized state of this cubic oxide.

Both hexagonal (h-WO_3) and pyrochlore (p-WO_3) oxides are built up of layers in which the WO_6 octahedra share their corners, forming six-membered rings (Figs. 1c and d). For h-WO_3, the stacking of these layers along the [001] axis leads to the formation of one-dimensional hexagonal tunnels along this direction [17], while in p-WO_3, these layers are stacked along the [111] direction, the layers being linked to each other by intermediate octahedra. This stacking leads to large three-dimensional hexagonal interconnected tunnels [18]. Their vibration spectra (Figs. 4a and 5a) show a maximum at 680 cm^{-1}. In addition, a small band at 800 cm^{-1} for h-WO_3 is noticeable. For p-WO_3 the small peak at 980 cm^{-1} is related to the presence of some W=O groups due to the fact that p-WO_3 is a lacunar oxide [18].

The hydrate $WO_3{\cdot}1/3\ H_2O$, precursor of h-WO_3, has a structure built up of the same kind of WO_6 layers as h-WO_3 with, however, one layer out of two shifted by a/2 along the [001] axis (Fig. 1e) [16]. This compound is characterized by two types of WO_6 octahedra: W1 where the six oxygen atoms connect the octahedra together by corner sharing, and W2 where two of the oxygen atoms are implicated in a short W=O bond and a longer W—OH_2 bond respectively, both bonds being along the [001] direction. This stacking leads to cavities, which are occupied by the structural water molecules. The monohydrate $WO_3{\cdot}1\ H_2O$ has a two-dimensional crystalline structure where each plane consists of WO_6 octahedra sharing four of their six corners in the ac plane (Fig. 1f) [26]. Across these planes, as in $WO_3{\cdot}1/3\ H_2O$, one oxygen forms part of a short W=O bond and the other belongs to a structural water molecule. The two-dimensional character of this hydrate results in the cohesion between each layer being brought about by hydrogen bonding. Their infrared spectra are presented in Figs. 6a and 7a for $WO_3{\cdot}1/3\ H_2O$ and $WO_3{\cdot}1\ H_2O$ respectively. In the ν(O—W—O) stretching mode range, both hydrates are characterized by a broad band

Table 1 Cell parameters of the different WO_3 phases before and after hydrogen intercalation

	Intercalation level, x	Cell type	Cell parameters (Å)	W—O distances (Å)	References
m-WO_3	0	monoclinic	a = 7.284(4) b = 7.507(4) c = 7.674(4) β = 90.62(4)	1.72–2.15	25
	0.23	tetragonal	a = 5.238(2) c = 3.891(3)		32
	0.33	tetragonal	a = 3.765(2) c = 3.732(2)		33
c-WO_3	0	cubic	a = 3.706(5)	1.86	
	0.35	cubic	a = 3.748(3)		
h-WO_3	0	hexagonal	a = 7.299(3) c = 7.796(5)	1.95, 1.89	17
	0.34	hexagonal	a = 7.374(2) c = 7.586(5)		
p-WO_3	0	cubic	a = 10.26(1)	1.97	18
	0.40	cubic	a = 10.295(8)		
$WO_3 \cdot 1H_2O$	0	orthorhombic	a = 5.246(3) b = 10.740(6) c = 5.127(2)	1.69 1.83, 1.93 2.34	26
	0.12	orthorhombic	a = 5.251(5) b = 10.62(2) c = 5.233(6)		
$WO_3 \cdot 1/3\ H_2O$	0	orthorhombic	a = 7.325(6) b = 12.56(1) c = 7.721(9)	(W1) 1.98, 1.96 2.02, 1.84 (W2) 2.11 2.51, 1.81	16
	0.08	orthorhombic	a = 7.348(6) b = 12.575(9) c = 7.717(9)		

centered around 700 and 660 cm^{-1} respectively, with, in addition for the monohydrate, a shoulder around 730 cm^{-1}. The positions of the infrared narrow peaks at 950 cm^{-1} for $WO_3 \cdot 1\ H_2O$ and at 1004 cm^{-1} and 960 cm^{-1} for $WO_3 \cdot 1/3\ H_2O$ due to the valence vibrations of the W=O groups [10] can be used as fingerprints for these hydrates.

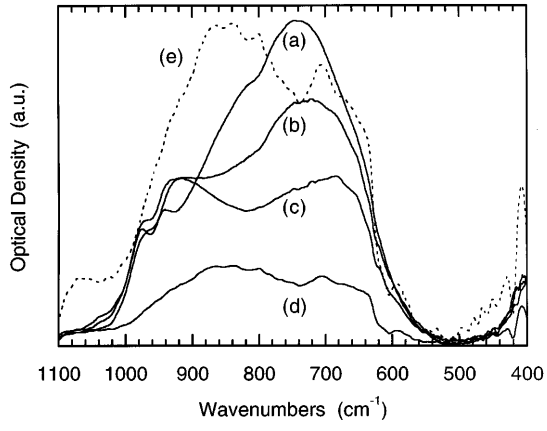

Fig. 3 Infrared spectra of cubic WO_3 (**a**) and of its H_xWO_3 bronzes with $x = 0.35$ (**d**) and intermediate hydrogen contents (**b** and **c**). Spectrum **e** corresponds to an amplification of **d** for convenient profile comparison with **a**

Table 2 Infrared vibration frequencies for WO_3 and $WO_3 \cdot x\ H_2O$ phases and their bronzes

	Intercalation level	ν(O—W—O) (cm^{-1})	ν(W=O) (cm^{-1})
m-WO_3	0	740 810	– –
	0.33	820 705	– –
c-WO_3	0	740	–
	0.35	850 710	– –
h-WO_3	0	680	–
	0.34	800 680	– –
p-WO_3	0	690	–
	0.40	700	–
$WO_3 \cdot 1\ H_2O$	0	660 740	950
	0.12	700	905
$WO_3 \cdot 1/3\ H_2O$	0	660	960 1004
	0.08	660	960 1004
a-$WO_3 \cdot 1\ H_2O$	0	695 880	960
	0.12	695 870	930

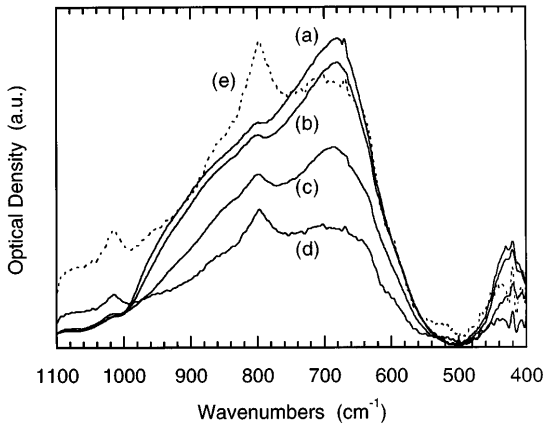

Fig. 4 Infrared spectra of hexagonal WO_3 (**a**) and of its H_xWO_3 bronzes with $x = 0.34$ (**d**) and intermediate hydrogen contents (**b** and **c**). Spectrum **e** corresponds to an amplification of **d** for convenient profile comparison with **a**

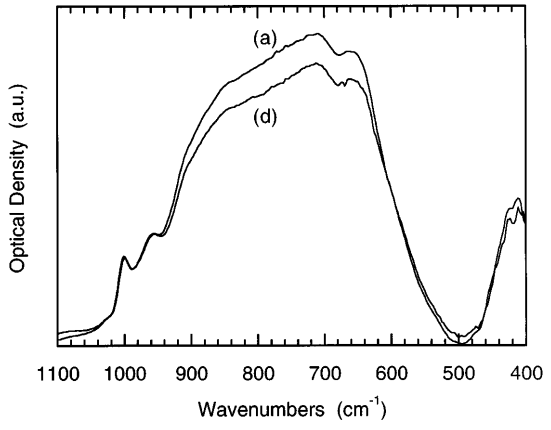

Fig. 6 Infrared spectra of $WO_3 \cdot 1/3\ H_2O$ (**a**) and of its bronze with $x = 0.08$ (**d**)

The last a-$WO_3 \cdot 1\ H_2O$ hydrate is considered amorphous (as determined from its X-ray diffractogram). The X-ray absorption spectroscopy study of this compound has shown three sets of W—O distances: two at 1.77 Å, two at 1.91 Å and two at 2.14 Å, implying highly distorted WO_6 octahedra [19]. The infrared spectrum consists of a broad band whose maxima (880 and 695 cm^{-1}) are located in the ν(O—W—O) range (Fig. 8a). Note that this spectrum differs from that of its crystallized precursor only by a shoulder around 960 cm^{-1}, while $WO_3 \cdot 1\ H_2O$ exhibits a well-defined peak characteristic of the ν(W═O) vibrations.

Hydrogen intercalation

The different oxides show a relatively high hydrogen content of about 0.35–0.40 per tungsten atom, in good agreement with a previous report [27]. Concerning the crystallized or amorphous hydrates, the intercalation level is much lower, about 0.12 for the crystallized and amorphous $WO_3 \cdot 1\ H_2O$, and still lower ($x = 0.08$) for $WO_3 \cdot 1/3\ H_2O$. It clearly appears that the hydrates and the oxides do not have the same capability with respect to hydrogen intercalation. This implies that structural water hinders hydrogen intercalation, while, as mentioned in the experimental section, adsorbed water favors this process.

The infrared spectra for different WO_3 reduced states are reported in Figs. 2–8. For a convenient comparison of band profiles, we have also represented by dashed lines the spectra obtained at the maximum x value multiplied by a factor which brings them at about the same intensity as those obtained at $x = 0$. The vibration frequencies are listed in Table 2.

A general trend is observed: the intensity of the spectra decreases when x increases. This can be explained by the transformation of the samples from an

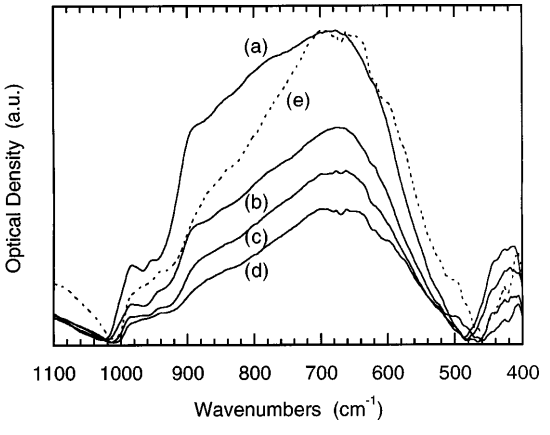

Fig. 5 Infrared spectra of pyrochlore WO_3 (**a**) and of its H_xWO_3 bronzes with $x = 0.40$ (**d**) and intermediate hydrogen contents (**b** and **c**). Spectrum **e** corresponds to an amplification of **d** for convenient profile comparison with **a**

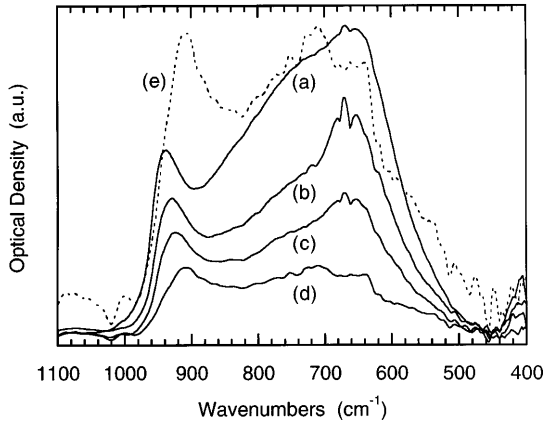

Fig. 7 Infrared spectra of monohydrate $WO_3 \cdot 1\ H_2O$ (**a**) and of its H_xWO_3 bronzes with $x = 0.12$ (**d**) and intermediate hydrogen contents (**b** and **c**). Spectrum **e** corresponds to an amplification of **d** for convenient profile comparison with **a**

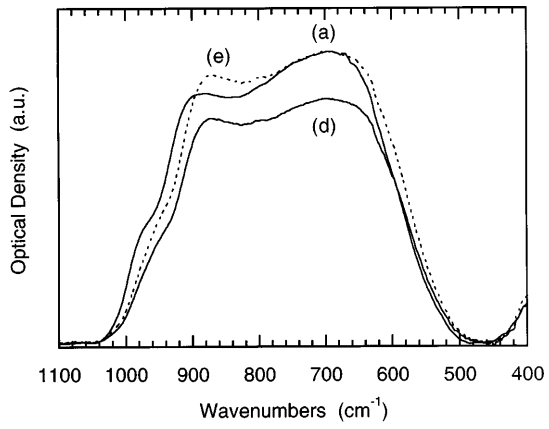

Fig. 8 Infrared spectra of amorphous hydrate $WO_3 \cdot 1\ H_2O$ (**a**) and of its bronze with x = 0.12 (**d**). Spectrum **e** corresponds to an amplification of **d** for convenient profile comparison with **a**

insulating to a quasi-metallic state. This strong increase in electronic conductivity is accompanied by a parallel increase in the reflectivity. Thus, when x increases, more and more infrared light is lost by reflection, causing a shielding effect on the measured signal. In addition, the mid-infrared spectra of inserted samples are situated on a sloping base line, which corresponds to the edge of the strong absorption centered in the visible. It is known that metallic behavior is more easily achieved in the crystalline than in the amorphous oxides at high x values. In crystalline oxides, the injected electrons are inserted into the conduction band of the tungsten atoms, creating an electronic cloud which is delocalized along the ordered structure. In amorphous materials, the inserted electrons are localized on the tungsten atoms as small polarons, and the reflectivity is less pronounced. From these general considerations, one can explain that for similar x values of about 0.12, the spectra of a-$WO_3 \cdot 1\ H_2O$ (Fig. 8) show less intensity attenuation than those of crystallized $WO_3 \cdot 1\ H_2O$ (Fig. 7). The spectra of the other oxides (Figs. 2–5) exhibit a marked intensity decrease when x varies from 0 to 0.33 or 0.40. However, crystallized $WO_3 \cdot 1/3\ H_2O$ does not exhibit a pronounced intensity decrease (Fig. 6), which can be related to its low intercalation content.

Behavior of m-WO_3, c-WO_3, h-WO_3, p-WO_3

If we consider the effect of the proton insertion on the spectra of the four oxides, it appears that at the maximum x value m- and c-WO_3 exhibit a similar profile composed of at least two components situated at about the same frequencies (Figs. 2d and 3d); the main broad sub-band is centered around 850 cm^{-1}. A second type of profile is reached by h- and p-WO_3, with a maximum at about 680–700 cm^{-1} and a secondary peak or shoulder at about 800–850 cm^{-1} (Figs. 4d and 5d). We believe that the first kind of profile can be associated with a three-dimensional arrangement of corner-sharing octahedra in a relatively symmetric ReO_3 type structure. The crystallographic data (Table 1) show clearly that m-WO_3 evolves, after insertion, towards a tetragonal structure with a = 3.76 Å and c = 3.73 Å, as has also been observed after electrochemical intercalation [28], whereas the cell parameter of c-WO_3 reaches the very similar value of 3.75 Å. The distribution of W—O distances is also expected to converge towards a mean value of about 1.86 Å. Thus, both spectroscopic and crystallographic results indicate that m-WO_3 looks more and more like the c-WO_3 phase after proton insertion. The same kind of reasoning applies to h- and p-WO_3, as these two compounds show the same type of six-membered corner-sharing octahedra. It can be seen that the profile of p-WO_3 has slightly changed from x = 0 to x = 0.40 (Fig. 5), in agreement with a small cell parameter variation from 10.26 Å to 10.30 Å, respectively (Table 1). The mean W—O distance is therefore expected to remain close to 1.97 Å. It is possible that the rather well-defined peak at about 850 cm^{-1} in h-WO_3 reflects the one-dimensional channel structure of this compound, disappearing in the three-dimensional channel structure of p-WO_3.

In a second step, if we consider each spectrum more specifically, m-, c-, and h-WO_3 show similar behavior when x increases from 0 to about 0.35. This can be described as an increase in an absorption band at high frequency which becomes more intense than the lower frequency component. In h-WO_3 the signals keep the same frequency during proton insertion (Fig. 4), while the cell parameters progressively change from 7.80 Å to 7.59 Å along the one-dimensional tunnels (c parameter) and perpendicularly from 7.30 Å to 7.37 Å (a parameter).

It must be pointed out that between the limiting cases x = 0 and $x = x_{max}$, the spectral variations are not linear. In all spectra, and particularly in the c- and p-WO_3 ones, weak bands or shoulders are present at x = 0 in the 900–1000 cm^{-1} range. According to the previously established correlations between frequencies and W—O bond lengths [29], these features correspond to rather short W—O bonds and even to terminal W═O groups. In principle, such bonds do not exist in three-dimensional cubic structures. Their presence has to be considered as indicative of defects in a poorly crystallized state, particularly in c-WO_3. They disappear when x increases, indicating that proton insertion removes these defects and systematically brings the oxides to more symmetric structures. As a general trend, frequency shift variations correspond to cell parameter variations. However, a small effect is produced in the cubic c-WO_3 as well as in p-WO_3 structures. With respect to the vibration changes, i.e. the appearance of a new band in c-WO_3 but no change in p-WO_3, only the basic arrangements of the WO_6 octahedra in the two cubic compounds can explain the different changes in their respective infrared spectra.

Behavior of $WO_3 \cdot 1\ H_2O$, $WO_3 \cdot 1/3\ H_2O$ and a-$WO_3 \cdot 1\ H_2O$

The three hydrates can contain much less inserted hydrogen than the oxides. Nevertheless, crystallized $WO_3 \cdot 1\ H_2O$ (Fig. 7) undergoes more important spectral changes than $WO_3 \cdot 1/3\ H_2O$ (Fig. 6) and a-$WO_3 \cdot 1\ H_2O$ (Fig. 8).

In $WO_3 \cdot 1\ H_2O$ (Fig. 7a), the two main components at 950 cm^{-1} and 670 cm^{-1} (with a shoulder at 730 cm^{-1}) are associated with the stretching frequencies of both the terminal W=O bonds and a distribution of W—O bonds, respectively (Table 1). After proton insertion, ν(W=O) is shifted to 905 cm^{-1}, and the second absorption becomes relatively weaker and broader, being centered at 700 cm^{-1}. Proton insertion produces again a more symmetric structure since the *c* and *a* parameters become nearly equal (Table 1). The *b* parameter changes from 10.74 Å to 10.62 Å, indicating a decrease in the interlayer distance. The orthorhombic symmetry is retained, due to the two-dimensional character of the crystalline structure. The spectral changes corroborate a re-distribution of the W—O distances. It is not possible, however, to know where the proton is located. Moreover, we have not reported the region of the stretching and bending vibrations of the water molecule, as the resolution of their respective bands was not good enough.

$WO_3 \cdot 1/3\ H_2O$ infrared spectra (Fig. 6) do not show any significant changes in the ν(O—W—O) region. The analysis of cell parameters (Table 1) does not show any variation either. This behavior could be due to its very low hydrogen content ($x_{max} = 0.08$). However, under a hydrogen atmosphere, this hydrate becomes light blue. This means that we must have only a surface intercalation process that is not strong enough to induce either structural or vibrational distortions. With regard to its crystalline structure, the stacking of the WO_6 layers does not indicate preferential intercalation channels. Furthermore, the cavities left by the stacking of these layers are occupied by the structural water molecules, making the hydrogen intercalation reaction difficult.

The infrared spectra of a-$WO_3 \cdot 1\ H_2O$, (Fig. 8) keep their original shape, and only minor changes appear after hydrogen intercalation, although the hydrogen content is equivalent to that of the crystallized hydrate ($x = 0.12$). Compared to its crystallized precursor, $WO_3 \cdot 1\ H_2O$, it exhibits a similar shift of the short bond vibration ν(W=O), although it is smaller (about 30 cm^{-1} vs 45 cm^{-1} in $WO_3 \cdot 1\ H_2O$). In the stretching vibration range, the changes are less pronounced and a little different. In fact, the relative intensities of the two main components in the 880–700 cm^{-1} range are not reversed after hydrogen intercalation. Thus, we can assume that the W—O bond variations are less important.

Discussion

The experimental results show that the effect of hydrogen intercalation on the WO_3-type materials as determined by X-ray diffraction and infrared measurements depends on both their structural features and their degree of crystallinity.

When the hydrogen intercalation reaction proceeds, electrons are inserted in the tungsten conduction band, leading to the partial reduction of the metal oxidation state from +VI to +V, the tungsten metal remaining surrounded by six oxygen atoms. During the intercalation step, some attractive interactions between the metal and the injected electrons may induce local distortions around the W^{+V} center, resulting in W^{+V}—O bonds being shorter than W^{+VI}—O bonds. According to the relationship between frequency and W—O bond length [29], a bond-shortening effect may be accompanied by shifts of some vibrations to higher frequency. In the c-WO_3 hydrogen bronzes, it can be estimated that some W—O bonds shorten from 1.85–1.90 Å in the non-intercalated state to about 1.70–1.75 Å . Before hydrogen intercalation, the W—O distance distribution in m-WO_3 is relatively large, from 1.72 Å to 2.15 Å [25]. After the reduction step, it may well be that a homogenization of the W—O distances occurs, leading to short W—O bonds of about 1.75 Å, since the infrared absorption band and the cell parameters are very close to those in the c-WO_3 bronzes. Such effects (shortening or redistribution of distances) need to be compensated by a W—O bond-lengthening effect to keep a mean W—O distance of 1.86 Å, thereby explaining either the evolution to a more symmetric tetragonal structure when intercalating hydrogen in m-WO_3 or the small increase in the cubic parameter for c-WO_3, where a shortening of the W—O bonds cannot by itself be responsible for its crystalline parameter variation. In infrared spectroscopy, such a lengthening would reveal itself by a shift to lower frequency, around 400–500 cm^{-1}. In h-WO_3, the cell parameter variation, $\Delta a = +0.07$ Å and $\Delta c = -0.21$ Å, shows a W—O shortening along the *c* direction in relation to the increase in the 800 cm^{-1} vibration band. Moreover, it may be that a light W—O lengthening occurs in the (110) plane, since the *a* parameter slightly increases. Furthermore, the distortion effects in a host structure can be explained according to the McKinnon theory [30], which has shown that the strain effects in intercalated systems are attractive along the intercalation channel and repulsive perpendicular to it. This theory applies very well to h-WO_3 and would confirm that the short W—O bonds observed by infrared spectroscopy should be favored along the *c* direction, which is consistent with the decrease in the *c* parameter. Moreover, this theory underlines the importance of the anisotropic character of a structure and led us to compare the hexagonal-type tunnelled structures. The infrared as well as the X-ray diffraction results confirm that the strains

induced by the intercalation reactions strongly depend on the structural isotropy of p-WO_3 and the structural anisotropy of h-WO_3.

Let us go through the behavior of the crystallized and amorphous $WO_3 \cdot 1\ H_2O$ hydrates. In the case of the crystallized monohydrate, the variations of the vibrations are slightly different as a result of the two-dimensional character of the structure. However, we can assume that the progressive change of the ν(O—W—O) vibrations (from a two-component band with one main maximum at 660 cm^{-1} and a shoulder at 730 cm^{-1} to a broader band with a medium frequency at 700 cm^{-1}) and the decrease in the ν(W═O) are both induced by the presence of the reduced state W^{+V}. The ν(O—W—O) band vibration corresponds to the 1.8–1.9 Å W—O bond. Since the *a* and *c* parameters become nearly equal, it is likely that there is homogenization of the W—O bonds in the *ac* plane. As the spectral distribution remains in the same frequency range and is centered at a medium frequency (700 cm^{-1}), the new W—O bond length distribution may stay around the same order of length , 1.8–1.9 Å. Furthermore, the decrease in the ν(W═O) frequency corresponds to an increase in the W═O bond length [29], from 1.69 Å [ν(W═O) = 950 cm^{-1}] to 1.72 Å [ν(W═O) = 905 cm^{-1}]. Relating this to the decrease in the *b* parameter, it seems likely that the cohesion by hydrogen bonds between the octahedron planes is reinforced after hydrogen intercalation. Consequently, the intercalated hydrogen should be attracted by the bridging O—W—O oxygens, in agreement with a previous report [8], since it is unlikely that the protons are located in the interlayer space because of either the reduction of the interlayer spacing or the terminal oxygens remaining involved in hydrogen bonds. The amorphous hydrate a-$WO_3 \cdot 1\ H_2O$ shows similar behavior with regard to the ν(W═O) vibration, although this is revealed by an infrared shoulder only. In the ν(O—W—O) range, no significant changes occur, consistent with the amorphous character of this compound.

As well as electrons, protons are inserted into the structure upon intercalation, maintaining electroneutrality in the materials. So, what are the effects of the presence of protons on the structure? Surprisingly, the present infrared experiments have not given any evidence of O—H groups, whatever the crystalline structures or the nature of the crystallized state. There can be several reasons for this. With respect to the infrared spectroscopy, we know that the O—H bonds have their stretching mode ν(O—H) around 3400 cm^{-1} and their bending mode δ(O—H) around 1600 cm^{-1} when in H_2O molecules, or around 3600 and 1200 cm^{-1} respectively if in M—O—H groups [8]. In our case, one could infer that these bands are hidden by the disappearance of the signal due to the metallic behavior of the bronzes. Furthermore, as tungsten bronzes are protonic conductors, the protons could be linked too weakly to the host structures, so that no O—H vibrations could be detected. A last possibility is that the proton is involved in rather strong OH–O bonds, giving very broad ν(O—H) and δ(O—H) absorptions, difficult to observe on a sloping base line. Some deuterium intercalation experiments have also been performed via an *in situ* deuterium intercalation process using the SPECAC hermetic cell. The goal was to show up specific vibration bands due to the substitution of intercalated hydrogen by intercalated deuterium. The different signals have kept the same shapes and positions. In the water vibration range, as for hydrogen intercalation, it was not possible to extract any specific information.

It is surprising that we could not pin down the bands associated with the protons, although they have been reported by several researchers. Up to now, we have no explanation for such a difference. However, with respect to the electronic charge of the oxygens, it is quite likely that the intercalated protons are themselves localized around the oxygens engaged in the W^{+V}—O_6 octahedron distortion. In the case of the hexagonal oxide structure, the slight increase in the *a* parameter is likely induced by a lengthening of W—O bonds inside the (010) plane. One can therefore believe that the intercalated protons will have a higher affinity for these oxygen atoms, which belong to distorted octahedra. Moreover, the ReO_3 type structures present three equivalent intercalation directions, and the intercalated protons may be localized around the distorted octahedra. As has been proposed for the bronze $H_{0.53}WO_3$ [4], these intercalated protons may have a high probability for being delocalized among several oxygens.

Although this study deals mainly with the crystalline phases, it is in agreement with the results obtained with thin films in [9]. From an infrared transmission study, these authors concluded that the hydrogen intercalation leads to W—O bond shortening and lengthening, corresponding to new absorption bands observed at 960 cm^{-1} and 570 cm^{-1} respectively. The intercalation mechanism was supposed to be of the small polaron type [31], implying that the inserted electron on a metal site produces a local disruption around the metal position and induces simultaneously shorter and longer metal oxygen bond around the same metal position. So, in the tungsten oxide bronzes, the intercalated protons would interact with the oxygen atoms engaged in the longer bond. As in our present work, they could not at any time detect the presence of the intercalated protons as W—O—H groups.

Conclusion

The present study shows that hydrogen intercalation in different polymorphic forms of tungsten oxides or hydrates induces distortions in the W—O skeleton as determined by infrared spectroscopy. These modifications are highly dependent on the ability of each compound to intercalate hydrogen. The m-, c- and h-WO_3 structures and the monohydrate $WO_3 \cdot 1\ H_2O$ are hardly

affected by the intercalation. The main effect observed is a change in the stretching vibrations, indicating a shortening of the W—O bonds in the oxides or a small redistribution of the W—O bonds in the monohydrate. Although the degree of intercalation is similar to that of the other oxides, p-WO_3 does not show any vibration modifications in relation to its crystalline structure, which includes large three-dimensional intercalation channels. Moreover, the lower intercalation content in the hydrates compared to the oxides was correlated with the presence of the structural water molecules. Because of the space they occupy in the crystalline structure, they reduce the hydrogen intercalation capacity. This explains why the hydrate $WO_3 \cdot 1/3\ H_2O$ presents a very low intercalation content which does not induce any distortions at all.

As already pointed out, several unsolved questions remain concerning the hydrogen intercalation mechanism, namely with respect to the detection of M—O—H groups. However, from the stretching mode ν(O—W—O) variations, we have indirectly deduced that the protons have a high probability of being located in the vicinity of the bridging oxygens.

References

1. Granqvist CG (1995) Handbook of inorganic electrochromic materials. Elsevier, Amsterdam
2. Yamada S, Yoshida S, Kitao M (1990) Solid State Ionics 40–41: 487
3. Habib MA, Maheswari SP (1991) J Electrochem Soc 138(7): 2029
4. Wiseman PJ, Dickens PG (1973) J Solid State Chem 6: 374
5. Dickens PG, Birtill JJ, Wright CJ (1979) J Solid State Chem 28: 185
6. Möller H, Müller-Warmuth W, Rüschendorf F, Schöllhorn R (1987) Z Phys Chem [NF] 151: 121
7. Wiseman PJ, Dickens PG (1976) J Solid State Chem 17: 91
8. Crouch-Baker S, Dickens PG (1986) Polyhedron 5(12): 63
9. Paul JL, Lassègues CJ (1993) J Solid State Chem 106: 357
10. Daniel MF, Desbat B, Lassègues JC, Gerand B, Figlarz M (1987) J Solid State Chem 67: 235
11. Freedman ML (1959) J Am Ceram Soc 81: 3834
12. Figlarz M (1994) Materials Science Forum 152–153: 55
13. Palatnik LS, Obol'yaninova OA, Naboka MN, Gladkikh NT (1973) Neorg Mater 9(5): 801
14. Yamaguchi O, Tomihisa D, Kawabata H, Shimizu K (1987) J Am Ceram Soc 70(5): C94
15. Zocher H, Jacobson K (1929) Koll Beich 28: 167
16. Gerand B, Nowogrocki G, Figlarz M (1981) J Solid State Chem 38: 312
17. Gerand B, Nowogrocki G, Guenot J, Figlarz M (1979) J Solid State Chem 29: 429
18. Coucou A, Driouiche A, Figlarz M, Touboul M, Chevrier G (1992) J Solid State Chem 99: 283
19. Laruelle S, Bouchet-Fabre B, Benazeth S, Michalovicz A (to be published)
20. Levy RB, Boudart M (1974) J Catal 32: 304
21. Gerand B, Figlarz M (1983) Spillover of Adsorbed Species, pp 275. Elsevier Science Publishers B.V., Amsterdam
22. Benson JE, Kohn HW, Boudart M (1966) J Catalysis 5: 307
23. Kiss BA, Tisza F (1980) Acta Chim Sci Hung 104: 211
24. Loopstra BO, Rietveld HM (1969) Acta Crystallogr B25: 1420
25. Loopstra BO, Boldrini P (1966) Acta Crystallogr 21: 158
26. Szymanski JT, Roberts AC (1975) Canadian Mineralogist 22: 681
27. Genin C, Driouiche A, Gerand B, Figlarz M (1992) Solid State Ionics 53–56: 315
28. Jarman RH, Dickens PG (1982) J Electrochem Soc 129: 2276
29. Cotton FA, Wing M (1964) Inorg Chem 4: 867
30. McKinnon WR, Hearing RR (1980) In: Murphy PW, Broadhead J, Steele BC (eds) Materials for advanced batteries. Plenum, New York
31. Schirmer OF, Wittwer V, Baur G, Brandt G (1977) J Electrochem Soc 124: 749
32. Dickens PG (1967) Hurditch Naturwissenschaften 215: 1266
33. Glemser N (1951) Z Anorg Allg Chem 265: 288